Optical and Quantum Electronics (2022) 54:488
https://doi.org/10.1007/s11082-022-03786-6

A comprehensive review on pulsed laser deposition technique to effective nanostructure production: trends and challenges

Adawiya J. Haider[1] · Taif Alawsi[2] · Mohammed J. Haider[3] · Bakr Ahmed Taha[4] · Haydar Abdulameer Marhoon[5,6]

Received: 14 March 2022 / Accepted: 28 April 2022

Abstract
Pulsed laser deposition (PLD) is a commonly utilized technology for growing thin films in academia and industry. Compared to alternative deposition processes, the PLD offers more excellent benefits such as adaptability, control over the growth rate, stoichiometric transfer, and an infinite degree of freedom in the ablation geometry. This investigation collected data from five reputable academic databases, including Science Direct, IEEE Xplore, Scopus, Web of Science, and Google Scholar. In this review, we analyzed and summarized 20 empiricals on the impact of pulsed laser deposition on the production nanostructure, including laser wavelength, laser fluence, repetition rate and pulse length of the laser pulse, pulse shaping of the laser spot, plasma generation, distance between substrates and target, angular position of the material, substrate temperature, gas composition, and target material properties. Finally, we show this field's advantages, challenges, and viewpoints and focus on the strengths and weaknesses that can improve the deposition of nanostructure properties for various applications. Therefore, provide fascinating insights into the interaction of these processes in different fields.

Keywords Pulsed laser deposition · Nanostructures · Nanocrystalline · Laser fluence · Substrate properties

Abbreviations

LPCVD	Low-pressure chemical vapor deposition
PECVD	Plasma enhanced chemical vapor deposition
ALD	Atomic layer deposition
PLD	Pulsed laser deposition
CHAP	Carbonated hydroxyapatite
MBE	Molecular beam epitaxy
CVD	Chemical vapor deposition

✉ Adawiya J. Haider
adawiya.j.haider@uotechnology.edu.iq

Extended author information available on the last page of the article

1 Introduction

Pulsed laser deposition (PLD) is a thin-film deposition technique that utilizes intense laser pulses to vaporize the target material. Particles that have been ablated exit the target and condense on the substrate. The deposition process is performed in a vacuum chamber to minimize particle dispersion. However, reactive gases are utilized to alter the deposit's stoichiometry in other instances (Gomes et al. 2017). As expansion fronts spread through the gas, their interactions with the plume create shock waves. Plasma generated by a laser is transitory and highly dependent on incident laser fluence (laser pulsed energy/spot area), laser wavelength, ambient gas composition, and pressure (Harilal et al. 2003). At the molecular level, design and manufacturing techniques are called to as "nanotechnology," which is derived from the Greek word nano, meaning "dwarf". Nanotechnology's most widely accepted definition is the manipulation, observing, and measuring of small objects on a nanoscale scale or smaller. Because of the variety of disciplines involved in nanotechnology's development, it is interdisciplinary (Fadhel et al. 2021).These fields include chemistry, physics, electrical engineering, materials science, and biosensors (Abood et al. 2022; Taha et al. 2020, 2021a, b; Taha 2021; Haider et al. 2017a; Kamaruddin et al. 2017; Arsad et al. 2011; Alkhabet et al. 2020; Kargozar and Mozafari 2018). Its unique structure determines special effects, including quantum dimensional, macroscopic quantum tunneling effects, optical, electrical, magnetology, and biology (Baig et al. 2021; Taha and Min 2022). The term "thin film" refers to a layer of material between nanometers and one micrometer in thickness. Nanoparticles are employed in many industries and are credited with advancements in energy generation, cutting instruments, optical coatings, and data storage. Thin layers are frequently to enhance the surface characteristics of materials. Transmission, reflection, absorption, hardness, abrasion resistance, corrosion, permeation, and electrical behavior of a bulk material surface can be enhanced by depositing a thin layer. Additionally, nanotechnology is based on thin-film technologies (Frey and Khan 2015; Treece et al. 1994). The thin film growth techniques used above can be broadly categorized as physical vapor deposition (PVD) or chemical vapor deposition (CVD). PLD provides more control over the deposition stoichiometry, making it the optimal technique for complicated deposition compositions. In addition, it has contributed significantly to materials research since 1987, spanning many complex material applications (Fujioka 2015; Venkatesan 2014). Since then, lasers have been widely applied in various of technical fields. Ablating the target substance is a complicated procedure. However, the laser pulse may penetrate the material's surface to a certain depth. This dimension is dictated by the laser wavelength and the refractive index of the target material and is typically in the 10 nm range. Within ten picoseconds for a nanosecond laser pulse, the solid electrical field is strong enough to remove electrons from the bulk of the penetrated volume (Hashida et al. 2009). PLD is a simple process that is conducted regularly. It has several remarkable qualities, including ablating a target material using a laser pulse delivered to a substrate and the serial growth of the created plasma plume. Despite the design's simplicity, the PLD process is fascinatingly intricate. The preceding process steps frequently overlap, are linked, and comprise many deposition parameters that may be adjusted and directly affect the characteristics of the thin films formed. These variables may include the target's composition, the laser wavelength, the pulse width, the spot size, the fluence, the background gas's design, the pressure, the distance between the target and the substrate, and the substrate temperature. The complex interplay of these interdependent deposition parameters enables the PLD user to deposit the film with the desired thickness and composition (Ojeda-G-P

et al. 2018). Due to the several processes involved, such as laser absorption, plume formation, and film growth, the PLD approach is exceedingly complicated, much more so at high pressures. These approaches yield a diverse array of nanoparticles and nanostructures with variable stoichiometric and size distributions. The methods and conditions used to create nanostructures are crucial if films with controlled composition, homogenous target, texture, surface topography, and stability in physiological environments are to be deposited. This review evaluates and analyzes the Pulsed Laser Deposition (PLD) factors affecting nanomaterials deposition and producing ZnO nanoparticle films.

2 Earlier background and recent developments

Pulsed lasers (PLDs) in film preparation have been one of the research hotspots in recent years because of the advancement of pulsed laser technology. When the ablation target is in a plasma, a plasma in a vacuum, or a background gas, pulse laser sputtering produces high energy peaks and small pulse widths. The expansion product allows PLD to deposit a specific component and a microtubular structure on a substrate layer when the substrate is expanded (Smith and Turner 1965; Al-Saedi et al. 2019; Atiyah et al. 2019). In 1987, researchers at Bell Laboratories discovered the Y–Ba–Cu–O film, which possessed high-temperature superconductivity, and people began to investigate the potential of PLD technology. Under this development, the value of PLD technology has increased. It is currently regarded as one of the most significant ways to make thin films today (Dijkkamp et al. 1987; Kuppusami and Raghunathan 2006; Abaas et al. 2020). These methods have demonstrated a marked improvement in the quality of ZnO thin films with O2 printing using the PLD method (Haider 2009). Titanium oxide (TiO_2) (Haider et al. 2018a), particles were deposited on glass and Si substrates over a temperature range of 100–400 °C in the PLD process with constant laser energy of 800 mJ and a frequency-doubled Nd: YAG laser wavelength of 532 nm at 10 Hz and pulse duration (Salih et al. 2019; Rashed et al. 2014; Daway Thamir et al. 2016; Haider et al. 2017b, c). PLD was used to create nanostructured ZnO thin films on quartz substrates. Temperatures of 400 to 600° C were used to study the effect on structural, optical, and dielectric characteristics (Afnan and Yousif 2011; Vinodkumar et al. 2018; Haider and Sultan 2018; Haider et al. 2019). The ablation process occurs when the target absorbs the laser energy, resulting in local fusion and removal, forming particles (Zhigilei 2003). This approach is used for all laser pulses in which emitted material occurs as vapor forms and clusters on the surface. Whenever PLD is used in a vacuum, the vapor particles are quickly deposited on the substrate and interact to form a film (Chen et al. 2004). On the other hand, if the vapor species is deposited at a higher pressure, it will collide with surrounding gas molecules many times, promoting the nucleation and growth of the particles before they reach the substrate (Checca et al. 2017). Hiroaki Nishikawa and colleagues published a few papers on the usage of PLDs at high pressures for CaP film deposition. The method used was an excimer laser at the pressures of up to 0.37 Torr with fluences of 0.7 J/cm, 1.4 J/cm, and 2.8 J/cm^2. They discovered that when CaP films are exposed to high pressures and fluences, they exhibit phosphorus deficiency (Nishikawa et al. 2018). CaP films were previously produced through PLD employing HA and doped-HA targets (Rau et al. 2014). It employs excimer laser sources such as ArF (193 nm) and KrF (248 nm) and a solid-state laser with 1064, 532, and 355 nm wavelengths. Depositions are generally performed at low laser fluence levels.

3 Laser—target interaction

A pulsed high-energy laser beam focuses on the target, material ablation. Thus, a dense layer of vapor accumulates in front of a target during phases of the laser pulse. Energy absorption boosts the pressure and temperature of this vapor over the length of the laser pulse, finally leading to partial ionization. Because of the tremendous pressure, this layer expands away from the target surface, resulting in the so-called plasma plume. During this expansion, internal heat and ionization energies are converted into kinetic energy (several hundred electron volts); the kinetic energy is muted by successive strikes as the ablated particles expand into a low-pressure background gas (Joe et al. 2017). The laser deposition process is often divided into two distinct parts. However, if we want to make an excellent film, the plasma plume should have exact stoichiometry as the target. If the target surface, for example, were consistently heated, absorbing light from a continuous-wave laser source would allow a significant percentage of the incoming power to be passed into the target's bulk. The surface's subsequent melting and evaporation would be primarily thermal. Because the target elements' melting temperatures and vapor pressures differed, they evaporated at various rates, resulting in a composition of the evaporated material that fluctuated over time and did not precisely match the target (Singh and Narayan 1989). The interaction between laser light and material occurs via photon absorption by electrons in the atomic system. Because of the absorbed energy, electrons are excited in high-energy states, which means that the material is heated to extremely high temperatures in a short period. The energy is then transferred to the grid via the electron subsystem via electron–phonon coupling. A multitude of elements influences the interaction of the laser beam with the target, including the absorption coefficient, the reflectivity of the target material, pulse frequency, wavelength, and laser fluence. Figure 1 explains and describes the steps of the laser interaction with the target material. $T(x,t)$ at every point in the material during the laser pulse is determined using the heat flow Eq. 1 (Singh and Narayan 1989).

$$\rho_i(T)C_{\rho i}(T)\frac{\partial T_i(x,t)}{\partial t} = \frac{\partial}{\partial x}\left(K_i(T)\frac{\partial T_i(x,t)}{\partial x}\right) + I_\circ(t)\{1-R(T)\}e^{-\alpha(T)x} \quad i=1,2 \qquad (1)$$

where x is the vector perpendicular to the target plane, t is the time, Cp(T) is the density and thermal heat capacity per unit mass, K is the thermal conductivity, and the subscript I denotes the solid conductivity and liquid phases, respectively. $R(T)$ and (T) are the target's reflection and absorption coefficients at the laser wavelength, respectively, and Io(t) is the laser intensity. The following heat flow equation is used to calculate the temperature,

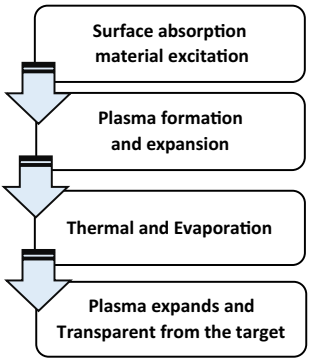

Fig. 1 The schematic describes steps in the interaction of laser pulses with the target material

$T(x,t)$, at any location in the material during the laser pulse. Assuming that heat conductivity is low on a nanosecond, the first component on the right side of this equation can be omitted. As a result, the goal surface temperature, x = 0, is given by Eq. 2 (Singh and Narayan 1989):

$$\rho(T)C_p(T)\left(T - T_0\right) = (1 - R)I_0\alpha(T)\tau \tag{2}$$

where T_0 is the starting temperature, τ is the duration of the pulse, even this very simplified equation still keeps the values, $\rho(T)$, $C_P(T)$, and $\propto (T)$ are functions of temperature and are not easy to determine. Thermal ablation can occur in three modes: vaporization, heterogeneous boiling, and explosive boiling; however, only vaporization and explosive boiling are compatible with the time scale of nanosecond laser pulses. Because explosive boiling occurs only when the target reaches temperatures close to the critical thermodynamic temperature of the material, the flow of material vaporized from the surface of a body at temperature T can be calculated using the Hertz-Knudsen Eq. 3, yielding an ablation rate given bySingh and Narayan (1989):

$$v_r(T) = (1 - \beta)\sqrt{\frac{m}{2\pi k_B T}}\frac{P_0}{\rho}\exp\left[\frac{L_V}{k_B}\left(\frac{1}{T_b} - \frac{1}{T}\right)\right] \tag{3}$$

Here T_b is the boiling temperature at pressure p_0, k_B is the Boltzmann constant, b is the backflow coefficient, and L_V is material's latent heat of vaporization.

4 Effects of nanomaterials deposition

A light beam passes via mirrors on a directed path before being focused into a vacuum chamber by a lens. In the chamber's low-pressure environment, the photons interact with the ablation target and convey energy to the material via the electrons of the target atoms, which are limited to a few tens to hundreds of nanometers in depth. Lambert's penetration depth is related to the laser wavelength's absorption coefficient, with smaller absorption coefficients resulting in greater penetration depths (Robert 2011). Both free and bound electrons may be stimulated, with some electrons being excited from the valence band to the conduction band while others being released instantly (non-thermal). The excited electrons transmit their energy to the grid in the order of picoseconds through an electron–phonon interaction and commence the thermal processes. A recent study showed that the role of laser fluence in the laser ablation process for the production of cobalt oxide nanoparticles in distilled water had been experimentally investigated. The output of a pulsed Nd: YAG laser was used to irradiate a high purity cobalt mass in distilled water. The laser had a wavelength of 1064 nm, a pulse width of 7 ns, and a repetition rate of 10 Hz. According to the findings, the laser energy significantly influenced the size and oxidation of the nanostructures produced (Ghaem et al. 2020). A schematic illustration of the laser deposition chamber setup, shown in Fig. 2, shows the positioning of the target and substrate holders within the chamber in relation to the laser beam.

4.1 Laser wavelength

The wavelength of the laser pulse has a strong influence on the deposition process. The following applies to ensure that atoms and ions are ejected without being heated: the shorter

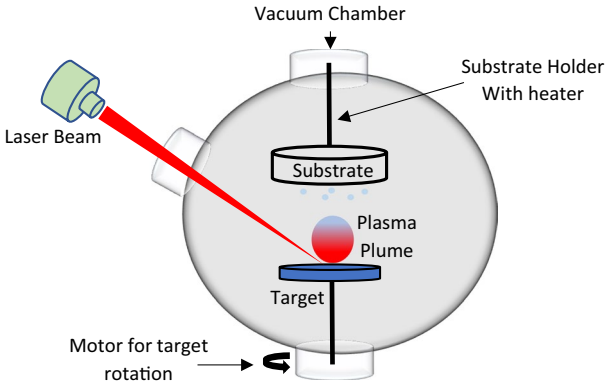

Fig. 2 Illustration of the pulsed laser deposition method in a vacuum

the wavelength, the higher the photon energy. The laser penetration depth is reduced due to shorter wavelengths, resulting in lower threshold fluences and faster ablation rates. The reduced concentration of nano/microparticles in UV radiation leads to denser particles and droplets than with longer wavelengths. The compositional deviations of a film can increase as a result. Typically, micro- and nanostructures are formed on the target surface during ablation, increasing the surface area and decreasing the effective laser fluence. Intriguingly, the wavelength affects the size and frequency of the periodic patterns formed on the target surface (Kautek 1990; Liu et al. 2004). The wavelengths affect both the absorbance through the material surface and the absorption by the laser plasma plume, with different wavelengths having a larger absorption capacity. Generally, the appropriate wavelength range for ablation is between 200 and 400 nm, most depositions are performed by excimer (157, 193, 222, 248, 308, and 351 nm) or Nd_3+: YAG lasers (266 or 355 nm).Excimers are frequently selected as ablation lasers because, compared to Nd: YAG lasers, which have a Gaussian energy profile with inherent fluence variation, have higher energies with a nearly flat upper energy profile. As a result, this variance is included in the deposition parameters. The effect of laser wavelength on characteristics of single-walled carbon nanotubes was reported. The method uses a double-pulse Nd: YAG laser operating at a wavelength of 355 or 1064 nm. The findings indicate that the useful range of ultraviolet laser radiation fluence is smaller. The characteristics of manufactured carbon nanotubes are significantly more reliant on laser fluence than on infrared laser radiation (Chrzanowska et al. 2015). Similar approaches have been used to investigate the effect of laser energy wavelength and energy, and the average size of gold nanoparticles generated using pulsed laser deposition is investigated (Jamaludin et al. 2020).

4.2 Laser fluence

Fluence is generally described in physics as the moment flux of a radiation or particle flow. In optics, the fluence F, for example, of a laser pulse, is the amount of optical energy supplied per unit area. Its most frequently used units are J/cm^2 (joules per square centimeter). Whenever a laser beam hits a target, the laser energy density is entirely determined by the laser pulse energy and the area of the target area. Equations 4 and 5 calculate the laser fluence and intensity (Dickey and Lizotte 2017).

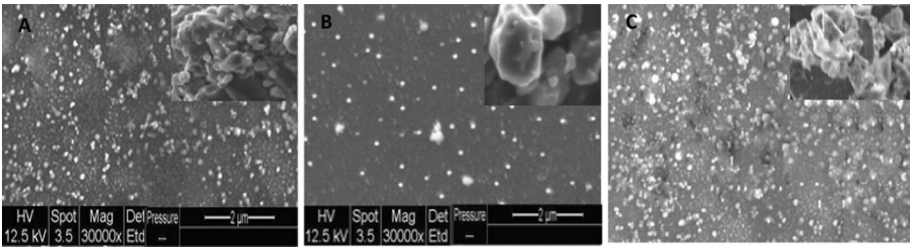

Fig. 3 SEM image of ZnO thin films deposited at different laser fluence energy densities: **a** 0.8 J/cm^2, **b** 1.6 J/cm^2, **c** 2.4 J/cm.^{2}

$$\text{Laser fluence } \left(\text{J/cm}^2\right) = \text{Laser energy (J)/beam area } \left(\text{cm}^2\right) \tag{4}$$

$$\text{Intensity} = (\text{Laser pulsed energy/pulse duration} \times \text{spot area}). \tag{5}$$

For a laser pulse to remove an atom from a target surface, the laser fluence must exceed the binding energy of the target material elements. As a result, the rate of ablation from the target is a function of laser fluence. The target's surface morphology, optical, transmittance, and electrical characteristics will be affected by laser fluence (Haider et al. 2021). Several studies have examined the effects of laser fluence on deposition, such Thin film of $BiFeO_3$ (Jaber et al. 2017), CuxS films' structural and optical characteristics (Rodríguez-Hernández et al. 2020), MgO film featuring nanostructures (Ismail et al. 2019; Prasad et al. 2013), as well as study the effect of laser fluence on the characteristics of produced ZnO thin films (Abdel-Fattah et al. 2018). However, fluency like the optical intensity, is a position-dependent variable. The fluency of a laser beam is frequently most significant towards the beam axis and diminishes somewhat away from it. Fluency is applicable only in conjunction with irradiation time for continuous wave beams. Figure 3 illustrated SEM images show the surface morphology of ZnO/Saphire films deposited under 5×10^{-2} mbar of oxygen gas at a substrate temperature of 400 °C. the films exhibit isolated ZnO aggregation with a size greater than (15.23) nm, which differs strongly from the surface of films with deposition at fluence laser energy 1.6 J/cm^2 and 2.4 J/cm^2.

4.3 Repetition rate and length of laser pulse

Most depositions in PLD have been carried out with nanosecond pulses. Since longer pulses often dominate thermal effects associated with droplet formation, femtosecond pulses (fs) frequently produce nanoparticles that may be exploited for various purposes (not thin layers such as defined here). Despite reports of picosecond (ps) or fs ablation being used to treat PLD are uncommon, there are few instances when fs ablation may be advantageous, for example, B. for diamond-like carbon coatings with a high sp3 concentration (Garrelie et al. 2006; Donnelly et al. 2010). An automatic laser processing system with adjustable pulse duration and an in-situ monitor that can collect more than 10,000 data points in a few hours has been developed. Authors have found that these parameters contribute most to the dependence of the laser ablation thresholds on the pulse duration, and it is a powerful tool that can contribute to understanding the mechanism of laser ablation. To accurately determine the expected value of the ablation threshold, it is important to increase the number of data points available for analysis (Takahashi et al. 2020). The

method used for the laser system was operated at a wavelength of 1050 nm with a repetition rate of 1 MHz and adjusted to the pulse duration from 0.53 to 31 ps.

4.4 Pulse shaping of the laser spot size

The change in the shape of the laser spot scattering on the target has an inverse influence on the plasma plume expansion with bigger laser spots resulting in a narrower and slow expansion and vice versa. However, utilizing an asymmetrical laser point, a specific consequence of this dynamic of plasma expansion occurs, known as the flip-over effect (Robert 2011). This reaction has been seen during both vacuum and high-pressure depositions and is most pronounced when the aspect ratio of the laser point is large (Al-Kinani et al. 2021; Schou et al. 2004; Ojeda-G-P et al. 2015a). A study showed Laser spot size Impact on ablation cone formation in polyethersulfone films. The method was a XeCl laser with a wavelength of 308 nm and fluences of 70 and 100 mJ /cm^2 in air. Materials were irradiated at two different laser spot sizes, w1 and w2 = 0.1 w1. It has been observed that the form, size, and volume of cones vary as the laser spot size changes. The number of pulses and the pulse repetition rate required for cone generation are also determined by the laser beam spot size on the surface (Pazokian et al. 2011). Research showed the effective spot size of excimer laser on ablation aluminum (Shaheen et al. 2016). Influence of spot size on the ablation morphology of aluminum alloys using a combined millisecond-nanosecond pulsed laser. The results show that the ablation morphology resembles a bowl when the nanosecond laser spot is larger, with minimal freezing at the edge. When the nanosecond laser spot is smaller, the ablation morphology resembles a hole, with the lump forming at the edge of the cavity (Yuan et al. 2018). However, the ablated material may be the significant source of droplets in metals or even particles generated by shock waves produced in the target during the laser ablation procedure. In the context of oxides, both negatively influence the quality of the thin layers deposited. Additionally, if ns pulses are utilized, various target materials may exhibit a range of thermal characteristics. Using Ps/fs pulses instead of plasma shielding can minimize these thermal effects and increase the ablation rate at high fluences. However, in conjunction with predicted plasma species, large amounts of unwanted nanoparticles are frequently found. The dispersion of material deposited on the substrate is related to the angular dispersion of the plasma plume that results. The breadth of the film thickness distribution may be defined as a dimensionless film width for a point source of material, as shown in Eq. 6 (Dickey and Lizotte 2017):

$$\Delta = \frac{X_{1/2}}{L} \tag{6}$$

where $X_{1/2}$ is the point coordinate at which the film's thickness equals half of its maximum value, and L is the distance between the substrate and the point source, this geometry. Figure 4 illustrates the effects of the pulse shape of the laser and spot size on the target for deposition. Laser power can be used on various materials, from metals and ceramics to biological materials, cells, and tissues. However, the material absorbs depending on the wavelength of the laser. For example, UV lasers are often used to machine polymers and other explicit materials in the visible spectrum but absorb ultraviolet. Femtosecond laser pulses, even transparent materials to the laser wavelength, may be machined in a reproducible and exact manner. Although the femtosecond laser pulse usually is in the infrared (800 nm, or 1060 nm).

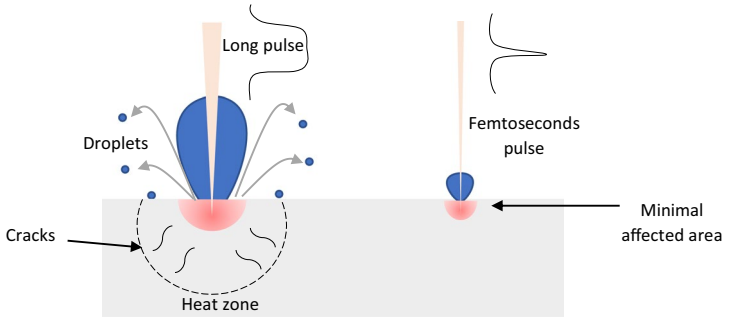

Fig. 4 Comparison of the effects between long pulse and femtosecond pulse laser

4.5 Plasma generation

Although its ns pulse still arrives, a plasma is generated above the target by a mixture of electronic (non-thermal) and vaporizing (thermal) ablation processes. Since plasma can absorb input photons, smaller photons are used for ablation. The plume spreads adiabatically at 30,000 m s1 and the species reaches a distance of 40 mm from the substrate in microseconds. Depending on the pressure of the gas in the environment and its type, it can interact chemically or elastically with surrounding gaseous molecules (Ojeda-G-P et al. 2017). An experiment showed a pulsed laser with a wavelength of 1064 nm and a repetition rate of 8.7 ns. The results revealed that the shock coupling coefficient varied with the laser fluence and that the coefficient decreased with increasing fluence due to the plasma shielding effect (Yu et al. 2020). Electron temperatures and electron number density are critical characteristics for comprehending laser-induced plasmas' properties. The optical emission spectrum is utilized to determine the electron temperature and number density using spectroscopy (Counselor and Burgum 1975).

4.6 Temperature of the substrate

The heating of the substrate has a significant effect on film development and surface shape since increased adatom mobility facilitates the production of crystalline films. The temperature of the substrate does not appear to affect how species enter the substrate directly, only how they exit. However, several studies have examined the effect of substrate temperature on plume growth (Li et al. 2006). The temperature of the substrate is critical in defining the structure of ZnO thin films grown on glass, quartz, and sapphire. Figure 5 illustrates the XRD data for different ZnO films produced at 300 °C, 400 °C, and 500 °C substrate temperatures (Al-Douri et al. 2016; Cropper 2018). At low temperatures, the crystalline size is smaller than at high temperatures. However, when the substrate temperature increases to 500 °C, the FWHM reduces, but the crystalline quality improves significantly compared to low temperatures. The FWHM of XRD is dependent on the crystallinity of each grain and the grain orientation distribution. The FWHM value is the reciprocal of the mean grain size; as the mean grain size grows, the FWHM value falls, indicating the film's optimum quality. Increasing the grain size and improving the crystal do not apply at elevated temperatures. We believe that it has two reasons: first, the film thickness is reduced, and

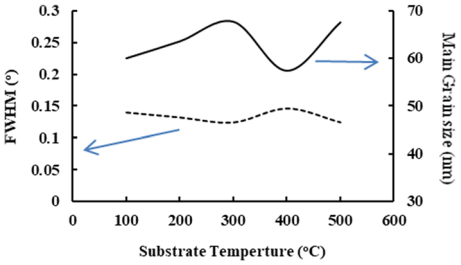

Fig. 5 Illustration of the temperature of the affected substrate. The main grain size and FWHM of ZnO (002) grown on glass at different substrate temperatures (Donnelly et al. 2010)

second, indeed, reflex (002) is caused by the nanostructure; it is perpendicular to the surface. However, they are smaller in size. The elevated temperature gives sufficient energy for the adatoms to achieve high surface mobility, hence favoring the production of sizeable columnar structure grains, as demonstrated by the SEM picture in Fig. 6.

4.7 Gas composition and pressure

The type and pressure of the gas mixture are considered essential for the successful deposition of a thin layer with the specified composition, thickness, and crystallinity. It is potentially one of the most key process factors, as it affects the kinetic energies of the species that arrive on the substrate, the incorporation of other components into the film, such as O from O_2, C from CH4 or N from NH_3, as well as the thickness of the film itself. Diagnostic tools such as ion probes, mass spectrometry, time and space resolved images, and laser-generated fluorescence are used to analyze the plume dynamics. The reason for this multi-technique methodology is the complicated composition of the organisms (Canulescu et al. 2009; Packwood et al. 2013; Sambri et al. 2016). Figure 7 illustrates the Surface morphology of the films deposited at a fixed substrate temperature of approximately 400 °C and oxygen pressure of 5×10^{-2} and 5×10^{-1} mbar. The method by which particles form is as follows. In the presence of gas, the mean free path of the substrate surface particles is decreased after initial expansion from the target surface. Notably, the higher the external pressure, the larger the number of collisions and scatterings. The particles then lose enough energy to form ionic combinations of molecules. If these aggregates reach the surface of the substrate, they develop into minute grains and constitute the nucleus. On the other

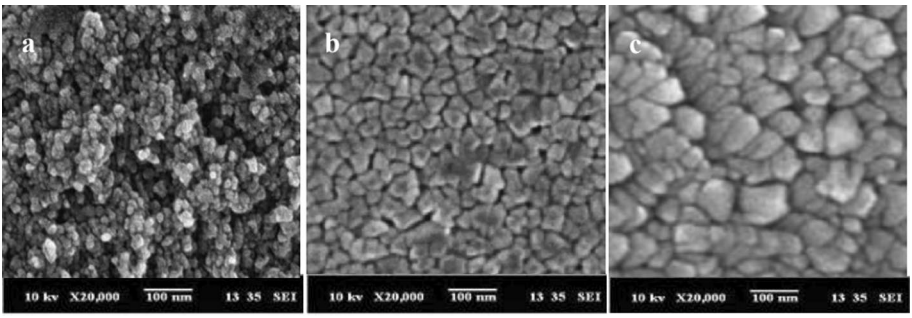

Fig. 6 SEM picture of ZnO thin films deposited at various temperatures: **a** 300 °C, **b** 400 °C, **c** 500 °C (Haider et al. 2018b; Cropper 2018)

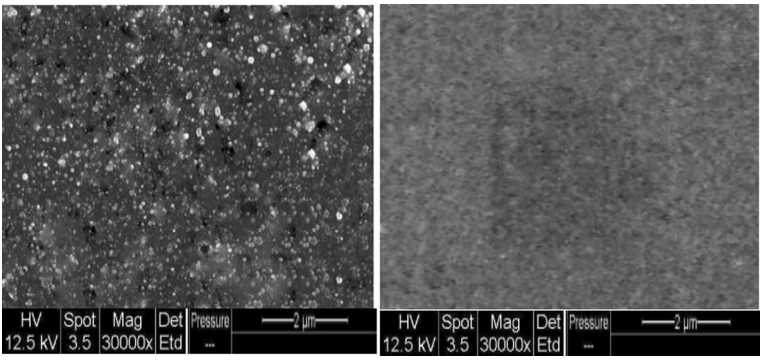

Fig. 7 SEM image of the ZnO thin films deposited at pressures varying from **a** 5×10^{-2} and **b** 5×10^{-1} mbar (Afnan and Yousif 2011; Haider et al. 2018b)

hand, if the ambient pressure is exceedingly low, most of the substrate surface particles can reach the substrate in a state close to that of single atoms.

4.8 Distance between substrates and target

The distance between the target and the substrate significantly affects the film thickness because it directly influences the solid angle of the plume expansion caught by the substrate. Increased distances result in a decrease in deposited material; for example, a 10 mm by 10 mm substrate positioned at 60 mm will collect only 25% of the species that a 30 mm × 30 mm substrate would capture, assuming no background gas is present. On the other hand, closer distances may cause a substantial species rebound due to extremely high kinetic energy exceeding 1000 eV. Furthermore, an increase in the target-to-substrate distance leads to a drop-in film thickness for distances greater than the mean free path of electrons (MFP) while operating under nonvacuum conditions. This is a direct consequence of the interactions between the plume species and the background gas. A study showed that the deposition rate increased as the range between substrate and target grew (Sangwaranatee et al. 2018).

4.9 Angular position of the material

PLD is a significantly forward-oriented deposition method that deposits most material within a 30° angular range under ordinary depositing circumstances. According to the forward-oriented aspect of the deposition, the angle of the substrate in relation to the plasma plume growth axis has a significant effect on the film thickness. Thus, small changes in angular location result in substantial decreases in film thickness. However, many researchers use At 45° incidence angles in laser deposition (Torrisi et al. 2001; Wang et al. 2004; Ojeda-G-P et al. 2015b).

4.10 Properties of target materials

Similarly, ablation effects are highly material-dependent. More specifically, different target materials will exhibit variable levels of laser absorption, resulting in differing ablation

rates. If we wish to build a film with the desired composition, the produced plasma plume should ideally have the exact stoichiometry as the target. For example, if the target surface is progressively heated, absorbing the light from a continuous-wave laser source, a large percentage of the incoming power can be directed into the target's bulk. The difference in melting points and vapor pressures of the target constituents would cause them to evaporate at different rates, resulting in a change in the composition of the evaporated material over time rather than the target. This incongruent evaporation produces films with stoichiometry significantly different from the aim (Counselor and Burgum 1975). Thus, the laser's energy must be rapidly discharged to the target surface to ensure congruent evaporation, avoiding considerable heat transmission into the confidential material. The melting and vaporization points of the target components are virtually simultaneously attained. The related high laser power density is obtained using a pulsed or Q-switched source focused on a tiny spot on the target. When the energy density is less than the ablation threshold, no material is removed, but some components may be deposited on the surface (Shen et al. 2004).

5 Critical analysis of studies

This section summarizes the analysis and summary of 12 empirical studies of critical literature on the fabrication of nanostructured pulsed laser deposition. A previous study by our group showed TiO_2/Ni composite as an antireflection coating for solar cells. The methodology was pure, and I-doped (1,3 & 5wt%) TiO_2 thin films were deposited using PLD techniques (Al-Kinani et al. 2020; Haider et al. 2016). Nanocrystalline cathode material $LiCo_{0.5}Ni_{0.45}Ag_{0.05}O_2$ (LCNAO) thin-film pulsed Nd-YAG laser with wavelength (532 nm) generated. Discovered that the energy gap of the LCNAO layers decreases from 4.2 to 3.8 eV when the substrate temperature increases from 100 to 300 °C. This means that the optical quality of the LCNAO layers has improved due to the increased crystal size and the decrease in defects in locations (Abaas et al. 2020; Haider et al. 2018c, 2020). A study showed the creation of a poison gas sensor from a WO_3 nanostructure by using PLD. The sensitivity was 80% at WO_3 dopant with Pt 5% (Fadhil et al. 2019). The produced Chromium oxide (Cr_2O_3) nanostructure was doped with Titanium oxide (TiO_2) thin films at varying concentration ratios of 3, 5, 7 and 9 wt% TiO_2 based on the PLD process (Kareem 2020). The nanostructure of calcium phosphate films produced by PLD in a high-pressure gas (argon) environment (1 Torr) utilizing infrared and green laser sources was examined. During 120 s, the plume created by an ablated hydroxyapatite target was deposited directly across transmission electron microscopy (TEM) grids (Checca et al. 2021). Thin vanadium pentoxide (V2O5) was produced with the PLD process based on a quartz glass substrate at temperatures ranging from ambient temperature to 300 °C (Farhan et al. 2021). Solar cells Cu_2ZnSnS_4 (CZTS) were studied using oxide, oxysulfide, and sulfide precursors synthesized by pulsed laser deposition. Consequently, a solar cell conversion efficiency of 5.4% has been reported for solar cells based on oxide precursors. This is the highest value reported so far for a PLD-produced CZTS absorber (Gansukh et al. 2020). The PLD technique in the evacuated chamber at 450° C was used to produce metal oxide thin films of the CdO structure and combine them with the ZnO structure (CdO/ZnO composite structure) (Mostafa and Menazea 2020). One of the exciting ways recently proposed in wound healing biomedical applications is the manipulation of nanofibrous formations that mimic the natural extracellular matrix by using PLD (Menazea et al. 2020a). Doping CuO into the thin film on the quartz substrate improved the catalytic activity for the degradation of

4-nitrophenol. The method used a PLD approach with a nanosecond Nd: YAG laser to improve the performance of the prepared CdO thin film, which is determined using a variety of spectroscopic techniques (Menazea et al. 2020b). PLD was used to create thin films of AlCrFeCoNiCu. At room temperature deposition, films display a mixture of FCC and BCC structures. Both crystal structures deteriorate with increasing deposition temperature, with the BCC deteriorating at a lower temperature than the FCC due to the loss of Al and Cu (Cropper 2018). A study discusses the use of pulsed laser deposition (PLD) to fabricate CdS thin films and CdS/Cu(In, Ga)Se_2 heterojunction structures on soda-lime glass (SLG) and Mo-coated SLG substrates under a variety of process parameters (Nicolaou et al. 2020). The authors describe the first effective heteroepitaxial development of Bi_2O_2Se films on $SrTiO_3$ substrates using the pulsed laser deposition (PLD) technique (Song et al. 2020). Table 1 refers to the deep analysis and summary of applied PLD for nanostructures produced from literature studies.

6 Key challenges and advantages

Despite the advantages mentioned above, laser processing of nanomaterials has significant disadvantages. Although laser microfabrication for shaping is significantly faster and less expensive than UV lithography, laser stamping and point-by-point exposure treatment are time-consuming and do not use parallel processing. In addition, laser processing makes it difficult to build three-dimensional nanostructures. The process is ideal for deposition on small substrates and yields high—quality films suitable for research and discrete devices. PLD technology has proven to be very effective and well suited to develop epitaxial films and enable the fabrication of multilayers, heterostructures and superlattices on lattice-matched substrates (Ursu et al. 2018). PLD enables films to grow in a highly reactive gas environment over various pressures. In the PLD process, suitable kinetic energy in the region of 10–100 eV and photochemical excitation exist during film growth compared to other deposition techniques and be beneficial for improving the quality of the deposited film. The main practical limitation of PLD is its relatively low duty cycle and incorporation of particles into the deposited films (Liu et al. 2021; Fiaschi et al. 2018). However, this is not unique to PLD as there are also particle problems in the case of sputtering and MOCVD. Complex oxide compositions with high melting points can be deposited quickly as long as the target materials absorb the laser energy. The target composition is transferred instantly, resulting in a stoichiometric separation. The turnaround time for the initial optimization of the growth conditions is much faster with this technique. This is always a great advantage when experimenting with different target compositions. Table 2 shows the advantages and challenges of Excimer and Nd: YAG lasers (Chaluvadi et al. 2021; Menazea and Awwad 2020).

7 Workflow and experimental setup

Nanostructures are well-known for their unique physical and chemical characteristics, making them ideal for various applications, including energy conversion and storage, nanoscale electronics, sensors and actuators, photonic devices, and even biological applications. Laser techniques have facilitated nanostructure preparation over the last decade, including hierarchical structure construction, patterning, heteroatom doping, and sputtering

Table 1 An analysis and summary of critical literature research on the use of PLD with nanostructures

Substrate	Laser wavelength (nm)	Laser fluence (J/cm^2) or energy mJ	Pulse duration (ns)	Repetition rate (Hz)	Gas pressure (mbar)	Substrate-target. distance (cm)	Temperature. °C	Band gap (eV)	References
Glass	Nd-YAG laser 532 nm	800 mJ	10 ns	6 Hz	Vacuum 2×10^{-5}	12 cm	299.85	3.82	Haider et al. (2016)
Glass	Nd-YAG laser 532 nm	1.4 J/cm^2	10 ns	1 Hz	10	1 cm	100, 200, 300	4.2–3.8	Haider et al. (2018c), Haider et al. (2020)
Glass and silicon	Nd-YAG laser 532 nm	1.6 J/cm^2	10 ns	1 Hz	10	0.4 cm	400	–	Fadhil et al. (2019)
Glass	360 nm,	700 mJ	NA	6 Hz	6–8	~2 cm	200	2.68–2.55	Kareem (2020)
Glass	IR (1064) Green (532)	76 J/cm^2	9 ns	10 Hz	1 Torr	30 ± 1 mm	25	–	Checca et al. (2021)
Silica	Excimer laser 308 nm	2.55 J/cm^2	10 ns	10 Hz	10^{-2}	4 cm	300	2.36–2.08	Farhan et al. (2021)
	Excimer laser 248 nm	2 J/cm^2	20 ns	15 Hz	10^{-6}	NA	540, 560,580	1.52–1.59	Gansukh et al. (2020)
Quartz	Nd-YAG laser 532 nm	NA	7 ns	10 Hz	NA	NA	450	3.91–3.95	Mostafa and Menazea (2020)
Quartz	1064 nm	NA	8 ns	10 Hz	4.5×10^{-5}	50 cm	50–60	–	Menazea et al. (2020a)
Quartz	1064 nm	NA	7 ns	10 Hz	10^{-4} Torr	50 cm	Room temp	2.41–3.39	Menazea et al. (2020b)
Glass	Nd-YAG laser 532 nm	2.0 Jcm-2	10 ns	10 Hz	2×10^{-10}	NA	Room temp	1.5	Cropper (2018)
SLG	excimer laser 248 nm	0.9–1.6 J/cm^2	~175 ps	10 Hz	4×10^{-6}	4 cm	25–300	2.55–2.49	Nicolaou et al. (2020)
Glass	Nd:YAG Q-switched (332 nm)	1.2 J/cm^2	7 ns	10 Hz	5×10^{-1}	4 cm	400	NA	Menazea et al. (2020a)

Table 1 (continued)

Substrate	Laser wavelength (nm)	Laser fluence (J/cm^2) or energy mJ	Pulse duration (ns)	Repetition rate (Hz)	Gas pressure (mbar)	Substrate-target. distance (cm)	Temperature. °C	Band gap (eV)	References
Glass	Nd:YAG	1.4 J/cm 2	7 ns	10 Hz	~1×10^{-3}	3 cm	27–300	NA	Menazea et al. (2020b)
Glass	Nd:YAG Q-switched (332 nm)	1.2 J/cm^2	7 ns	10 Hz	10^{-1} Torr	NA	200–500	3.6 eV	Cropper (2018)
Glass	Nd:YAG Q-switched (332 nm)	(0.5–1) J/cm^2	7 ns	10 Hz	~1 × 10–3	3 cm	100–200	NA	Nicolaou et al. (2020)
Glass	Nd:YAG (1064 nm)	(1000–500) mJ	15 ns	1 Hz	NA	1 cm	27	NA	Song et al. (2020)
Glass	Nd:YAG (332 nm)	0.4 J/cm^2	7 nm	10 Hz	10^{-3} Torr	3 cm	400	3.59–3.32 eV	Ursu et al. (2018)
Glass	Nd:YAG Q-switched (332 nm)	0.8 J/cm^2	10 ns	10 Hz	10^{-1} Torr	5 cm	200–400	3.51 eV	Liu et al. (2021)

Table 2 Performance features of Excimer and Nd: YAG lasers

Laser type	Advantages	Challenges	Key references
Excimer laser	High output power Strong stability Tuning adaptability Laser output adjustment	Limited operational life Complicated Maintenance Extensive and high-purity gasses, with continuous replenishing Space consuming	Ursu et al. (2018), Liu et al. (2021), Fiaschi et al. (2018)
Nd: YAG laser	Sufficient output energy for pulsed laser deposition Easy to maintain Compact system	Large energy reductions for the 3rd harmonic mode	Chaluvadi et al. (2021), Menazea and Awwad (2020)

etching (Zhao et al. 2021). Furthermore, laser-assisted material processing can be divided into two types: nonreactive thermal processing and reactive chemical processing. Thermal processing is simply a heat treatment performed in a vacuum or other environment. Every chemical reaction involves an activation or intensification (Herziger and Kreutz 1989). In the synthesis of nanomaterials by laser, the basic processing principle is that the absorption of the laser radiation generates the photothermal and/or photochemical impacts that promote the transformation and crystallization of the precursor materials. The desired thermal or chemical effect can be set by modifying the laser procedure parameters such as sampling rate, pulse width, and laser fluence (Hong et al. 2016; Dong et al. 2019). As a result, the laser wavelength is determined by the light absorption characteristics of the precursor materials. Additionally, combining cold-laser processing with thermal laser synthesis enables the fabrication of more advanced circuits with finely defined patterns and functionalization. As a result of the rapid advancement of laser processing technology, further applications based on nanomaterials will be investigated. Production can be accomplished by combining and digitizing laser process parameters with computer design and a manufacturing system. Finally, due to the benefit of precise control over the laser process, in situ synthesis or in situ sputtering etching may be tuned to maintain precursor morphology following laser processing by modifying laser focus distance (Joe et al. 2017; Rodkey et al. 2021; Lu et al. 2021; Ogugua et al. 2020; Fenech and Sharma 2020).

Figure 8 illustrates the workflow standards to be considered during the deposition process by PLD. Thus, laser synthesis and microfabrication are complementary. Promising procedures for nanomaterials and nanostructures development for a variety of purposes.

7.1 Prospective and advanced applications

The technical demand for devices with specific features based on multilayers, interfaces with atomic-level control, strained layers, and so on has paved the way for PLD to transition from a pure research laboratory-based approach to an industrially relevant instrument. This change is supported once again by PLD firms' instrumental innovations, which enable massive area deposition on wafers of up to 200 mm diameter that meets industrial requirements. More excellent knowledge of the process and technological advancements evolved into a flexible thin-film deposition that now competes with the traditional molecular beam epitaxy (MBE) technique for the controlled deposition of high-quality oxide layers. In addition, the laser light focuses on a narrow zone

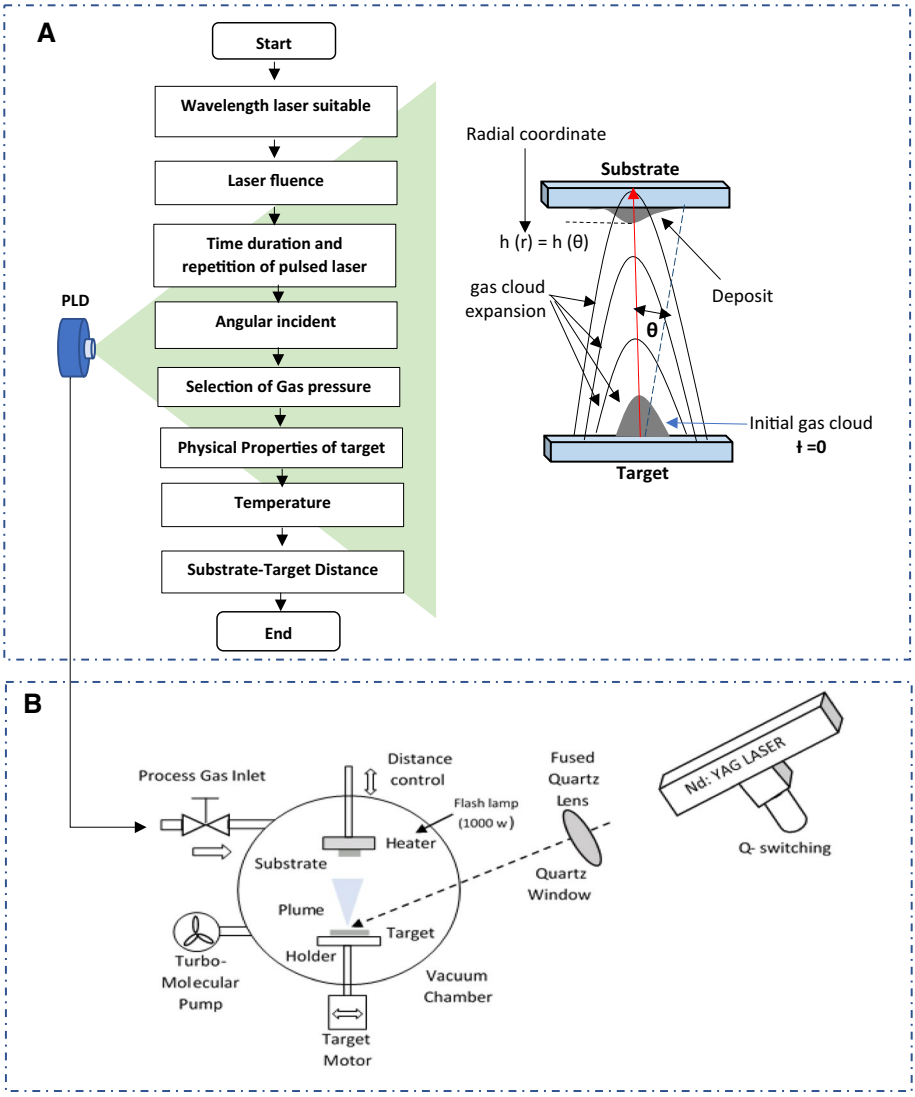

Fig. 8 Scheme of pulsed laser deposition for nanoparticles production: **a** workflow of PLD; **b** experimental set-up of our work

on the target surface, resulting in excellent process efficiency, control, and flexibility. Transfer can be from bulk to thin film under specific experimental conditions, as in the case of superconductors with high critical temperatures of piezoelectric and ferroelectric compounds. Table 3 shows the description of the advanced application using PLD.

Table 3 Advanced applications

Films	Advanced applications	Type of substrate	Laser wavelength (nm)	Key features	References
CHAP/Au	Biomedical	Quartz	1064 nm	Controlling the content of the coating might have a significant impact on the biological response	Ahmed et al. (2020)
$BaTiO_3$ (BTO)	Ferroelectric thin films	Silicon	248 nm	Dielectric and electromechanical properties combined	Lyu et al. (2018)
$Ga_{0.6}Fe_{1.4}O_3$	Multiferroic thin films	Single-crystal	248 nm	Manipulate magnetic domain structures on a large scale	Zhang et al. (2021)
$PbTiO_3/PbZrO_3$	Superlattices	Single-crystal	0.1542 nm	Improved the ferroelectric and dielectric characteristics and was lowered leakage current density	Lin et al. (2018)
$Sr_2V_2O_7$ (SVO)	Conducting thin films for electrodes	Single crystals	248 nm	Characteristics improved, such as electrical conductivity and carrier mobility	Mirjolet et al. (2019)

8 Conclusions

Due to the technique's simplicity, PLD is commonly utilized in research laboratories to develop thin films, ablation, deposition, etc. Additionally, it shows great promise for various commercial applications such as coated-conductor, microwave filter, solar cell, sensors, and satellite communication. PLD has a high-power density laser with a narrow, wide bandwidth to vaporize the appropriate substance. This procedure is mainly employed when previous techniques such as LPCVD, PECVD, and ALD have proven difficult or have failed to deposit the material. In conclusion, PLD makes it very easy to generate multicomponent films with the required stoichiometric ratio, a rapid deposition rate, a short test duration, and a low substrate temperature as a requirement. It is adaptable and has significant development potential and compatibility. In addition, atoms arrive in clusters, which enables much more accurate deposition. Thus, increasing growth control (e.g., by altering laser settings). Finally, PLD generates plasma using a UV pulsed laser with a high photon capacity and energy density, making it non-polluting as well as easy to handle.

Acknowledgements The authors gratefully acknowledge the financial and technical support provided by the Applied Sciences Department, university of technology, Baghdad, Iraq, and Al-Ayen University, Thi-Qar, Iraq.

Author contributions A.J.H. and B.A.T, Conceptualization and methodology, M.J.H., wrote the initial manuscript draft. With the support of T.A. and H.A.M., all authors have reviewed and accepted the published version of the manuscript.

Funding Not applicable.

Data availability Not applicable.

Declarations

Conflict of interest The authors declare no conflict of interest.

Ethics and permission to participate This manuscript has not been previously published and is not currently being considered by any journal for publication.

Institutional review board statement Not applicable.

Informed consent Not applicable.

References

Abaas, R.A.R., Haider, A.J., Jabbar, F.A., Hathal, M.M.: Characterisation of Fe doped layered cathode material as nano-rechargeable batteries. IOP Conf. Ser. Mater. Sci. Eng. **987**, 012011 (2020). https://doi.org/10.1088/1757-899X/987/1/012011

Abdel-Fattah, E., Elsayed, I.A., Fahmy, T.: Substrate temperature and laser fluence effects on properties of ZnO thin films deposited by pulsed laser deposition. J. Mater. Sci. Mater. Electron. **29**, 19942–19950 (2018). https://doi.org/10.1007/s10854-018-0124-8

Abood, M.S., Hamdi, M.M., Taha, B.A., et al.: Performance of effect for XPM and FWM in fiber optics. Lect. Notes Netw. Syst. **322**, 345–355 (2022). https://doi.org/10.1007/978-3-030-85990-9_29

Afnan, K., Yousif, A.J.H.: Effect of substrate temperature on microstructural and optical properties of ZnO films grown by pulsed laser deposition. Eng. Technol. J. **29**, 58–64 (2011). https://doi.org/10.1016/S1001-0521(06)60033-8

Ahmed, M.K., Ramadan, R., Afifi, M., Menazea, A.A.: Au-doped carbonated hydroxyapatite sputtered on alumina scaffolds via pulsed laser deposition for biomedical applications. J. Market. Res. **9**, 8854–8866 (2020). https://doi.org/10.1016/j.jmrt.2020.06.006

Al-Douri, Y., Haider, A.J., Reshak, A.H., et al.: Structural investigations through cobalt effect on ZnO nanostructures. Optik **127**, 10102–10107 (2016). https://doi.org/10.1016/j.ijleo.2016.08.012

Alkhabet, M.M., Girei, S.H., Paiman, S., et al.: Highly sensitive hydrogen sensor based on palladium-coated tapered optical fiber at room temperature. 8186 (2020). https://doi.org/10.3390/ecsa-7-08186

Al-Kinani, M.A., Haider, A.J., Al-Musawi, S.: High uniformity distribution of Fe@Au preparation by a micro-emulsion method. IOP Conf. Ser. Mater. Sci. Eng. **987**, 012013 (2020). https://doi.org/10.1088/1757-899X/987/1/012013

Al-Kinani, M., Haider, A., Al-Musawi, S.: Study the effect of laser wavelength on polymeric metallic nanocarrier synthesis for curcumin delivery in prostate cancer therapy: in vitro study. J. Appl. Sci. Nanotechnol. **1**, 43–50 (2021). https://doi.org/10.53293/jasn.2021.11023

Al-Saedi, S.I., Haider, A.J., Naje, A.N., Bassil, N.: Improvement of Li-ion batteries energy storage by graphene additive. Energy Rep. **6**, 64–71 (2019). https://doi.org/10.1016/j.egyr.2019.10.019

Arsad, N., Li, M., Stewart, G., Johnstone, W.: Intra-cavity spectroscopy using amplified spontaneous emission in fiber lasers. J. Lightwave Technol. **29**, 782–788 (2011). https://doi.org/10.1109/JLT.2010.2103048

Atiyah, A.A., Haider, A.J., Dhahi, R.M.: Cytotoxicity properties of functionalised carbon nanotubes on pathogenic bacteria. IET Nanobiotechnol. **13**, 597–601 (2019). https://doi.org/10.1049/iet-nbt.2018.5394

Baig, N., Kammakakam, I., Falath, W., Kammakakam, I.: Nanomaterials: a review of synthesis methods, properties, recent progress, and challenges. Mater. Adv. **2**, 1821–1871 (2021). https://doi.org/10.1039/d0ma00807a

Canulescu, S., Papadopoulou, E.L., Anglos, D., et al.: Mechanisms of the laser plume expansion during the ablation of $LiMn_2O_4$. J. Appl. Phys. **105**, 063107 (2009). https://doi.org/10.1063/1.3095687

Chaluvadi, S.K., Mondal, D., Bigi, C., et al.: Pulsed laser deposition of oxide and metallic thin films by means of Nd:YAG laser source operating at its 1st harmonics: recent approaches and advances. J. Phys. Mater. **4**, 032001 (2021). https://doi.org/10.1088/2515-7639/abe661

Checca, N.R., Caraballo-Vivas, R.J., Torrão, R., et al.: Phase composition and growth mechanisms of half-metal Heusler alloy produced by pulsed laser deposition: from core-shell nanoparticles to amorphous randomic clusters. Mater. Chem. Phys. **196**, 103–108 (2017). https://doi.org/10.1016/j.matchemphys.2017.04.037

Checca, N.R., Borghi, F.F., Rossi, A.M., et al.: Nanostructure of calcium phosphate films synthesized by pulsed laser deposition under 1 Torr: effect of wavelength and laser energy. Appl. Surf. Sci. **545**, 148880 (2021). https://doi.org/10.1016/j.apsusc.2020.148880

Chen, X.Y., Lu, Y.F., Wu, Y.H., et al.: Optical properties of SiO_x nanostructured films by pulsed-laser deposition at different substrate temperatures. J. Appl. Phys. **96**, 3180–3186 (2004). https://doi.org/10.1063/1.1782274

Chrzanowska, J., Hoffman, J., Małolepszy, A., et al.: Synthesis of carbon nanotubes by the laser ablation method: Effect of laser wavelength. Phys. Status Solidi B Basic Res. **252**, 1860–1867 (2015). https://doi.org/10.1002/pssb.201451614

Counselor, T., Burgum, L.: Spectral line broadening by plasmas. Sch. Psycol. Rev. **32**, 1975 (1975)

Cropper, M.D.: Thin films of AlCrFeCoNiCu high-entropy alloy by pulsed laser deposition. Appl. Surf. Sci. **455**, 153–159 (2018). https://doi.org/10.1016/j.apsusc.2018.05.172

Daway Thamir, A., Haider, A.J., Ali, G.A.: Preparation of nanostructure TiO_2 at different temperatures by pulsed laser deposition as solar cell. Eng. Technol. J. **4**, 3 (2016)

Dickey, F.M., Lizotte, T.E.: Laser Beam Shaping Applications, 2nd edn. CRC Press, Boca Raton (2017)

Dijkkamp, D., Venkatesan, T., Wu, X.D., et al.: Preparation of Y–Ba–Cu oxide superconductor thin films using pulsed laser evaporation from high Tc bulk material. Appl. Phys. Lett. **51**, 619–621 (1987). https://doi.org/10.1063/1.98366

Dong, W., Liu, H., Behera, J.K., et al.: Wide bandgap phase change material tuned visible photonics. Adv. Funct. Mater. **29**, 1–9 (2019). https://doi.org/10.1002/adfm.201806181

Donnelly, T., Lunney, J.G., Amoruso, S., et al.: Angular distributions of plume components in ultrafast laser ablation of metal targets. Appl. Phys. A Mater. Sci. Process. **100**, 569–574 (2010). https://doi.org/10.1007/s00339-010-5877-8

Fadhel, M.M., Ali, N., Rashid, H., et al.: A review on rhenium disulfide: synthesis approaches, optical properties, and applications in pulsed lasers. Nanomaterials **11**, 2367 (2021). https://doi.org/10.3390/nano11092367

Fadhil, F.A., Sultan, F.I., Haider, A.J., Rsool, R.A.: Preparation of poison gas sensor from WO_3 nanostructure by pulsed laser deposition. AIP Conf. Proc. **2190**, 020056 (2019). https://doi.org/10.1063/1.5138542

Farhan, M.S., Salim Alrikabi, H.T.H., Abed, F.T.: Impact of substrate temperatures on the properties of V_2O_5 thin films deposited by pulsed laser deposition. J. Phys. Conf. Ser. **1973**, 012074 (2021). https://doi.org/10.1088/1742-6596/1973/1/012074

Fenech, M., Sharma, N.: Pulsed laser deposition-based thin film microbatteries. Chem. Asian J. **15**, 1829–1847 (2020). https://doi.org/10.1002/asia.202000384

Fiaschi, G., Mirabella, S., Franzò, G., et al.: Effect of laser annealing on ZnO nanorods grown by chemical bath deposition on flexible substrate. Appl. Surf. Sci. **458**, 800–804 (2018). https://doi.org/10.1016/j.apsusc.2018.07.092

Frey, H., Khan, H.R.: Handbook of Thin-Film Technology, pp. 1–379. Springer, Berlin (2015). https://doi.org/10.1007/978-3-642-05430-3

Fujioka, H.: Pulsed Laser Deposition (PLD), 2nd edn. Elsevier, Amsterdam (2015)

Gansukh, M., López Mariño, S., Espindola Rodriguez, M., et al.: Oxide route for production of Cu_2ZnSnS_4 solar cells by pulsed laser deposition. Sol. Energy Mater. Sol. Cells **215**, 110605 (2020). https://doi.org/10.1016/j.solmat.2020.110605

Garrelie, F., Donnett, C., Loir, A.S., Benchikh, N.: New trends in femtosecond pulsed laser deposition and femtosecond produced plasma diagnostics. High-Power Laser Ablation VI **6261**, 179–187 (2006). https://doi.org/10.1117/12.669122

Ghaem, E.N., Dorranian, D., Sari, A.H.: Characterization of cobalt oxide nanoparticles produced by laser ablation method: effects of laser fluence. Physica E **115**, 113670 (2020). https://doi.org/10.1016/j.physe.2019.113670

Gomes, G.C., Borghi, F.F., Ospina, R.O., et al.: Nd:YAG (532 nm) pulsed laser deposition produces crystalline hydroxyapatite thin coatings at room temperature. Surf. Coat. Technol. **329**, 174–183 (2017). https://doi.org/10.1016/j.surfcoat.2017.09.008

Haider, A.J.: An interesting experimental observation of O_2 pressure effect on the surface roughness of ZnO thin films prepared by PLD technique. Iraqi J. Appl. Phys. Lett. **2**, 3–4 (2009)

Haider, A.J., Sultan, F.I.: Structural, morphological and random laser action for dye-Zno nanoparticles in polymer films. Int. J. Nanoelectron. Mater. **11**, 97–102 (2018)

Haider, A.J., Najim, A.A., Muhi, M.A.H.: TiO_2/Ni composite as antireflection coating for solar cell application. Opt. Commun. **370**, 263–266 (2016). https://doi.org/10.1016/j.optcom.2016.03.034

Haider, A.J., Haider, M.J., Majed, M.D., et al.: Effect of laser fluence on a microarray droplets micro-organisms cells by LIFT technique. Energy Procedia **119**, 256–263 (2017a). https://doi.org/10.1016/j.egypro.2017.07.078

Haider, A.J., Thamir, A.D., Najim, A.A., Ali, G.A.: Improving efficiency of TiO_2:Ag/Si solar cell prepared by pulsed laser deposition. Plasmonics **12**, 105–115 (2017b). https://doi.org/10.1007/s11468-016-0235-0

Haider, A.J., Al-Anbari, R.H., Kadhim, G.R., Salame, C.T.: Exploring potential environmental applications of TiO_2 nanoparticles. Energy Procedia **119**, 332–345 (2017c). https://doi.org/10.1016/j.egypro.2017.07.117

Haider, A., Al-Anbari, R., Kadhim, G., Jameel, Z.: Synthesis and photocatalytic activity for TiO_2 nanoparticles as air purification. MATEC Web Conf. **162**, 1–6 (2018a). https://doi.org/10.1051/matecconf/201816205006

Haider, A.J., Yousf, A.K., Shakir, A.K., et al.: Effect of laser energy density on ZnO/α-Al_2O_3 of films grown by pulsed laser deposition. Iraqi Laser Sci. J. **1**, 12–21 (2018b)

Haider, A.J., Al-Rsool, R.A., Al-Tabbakh, A.A., et al.: Structural, morphological and optical properties of $LiCo_{0.5}Ni_{0.45}Ag_{0.05}O_2$ thin films. AIP Conf. Proc. **1968**, 020001 (2018c). https://doi.org/10.1063/1.5039160

Haider, A.J., Sultan, F.I., Haider, M.J., Hadi, N.M.: Spectroscopic and structural properties of zinc oxide nanosphere as random laser medium. Appl. Phys. A **125**, 1–10 (2019). https://doi.org/10.1007/s00339-019-2529-5

Haider, A.J., Rsool, R.A.R.A., Haider, M.J., et al.: Properties of $LiCo_{0.5}Ni_{0.45}Ag_{0.05}O_2$ thin films for high storage energy capacity by pulsed laser deposition. Energy Rep. **6**, 85–94 (2020). https://doi.org/10.1016/j.egyr.2020.08.028

Haider, A.J., Jabbar, A.A., Ali, G.A.: A review of pure and doped ZnO nanostructure production and its optical properties using pulsed laser deposition technique. J. Phys. Conf. Ser. **1795**, 012015 (2021). https://doi.org/10.1088/1742-6596/1795/1/012015

Harilal, S.S., Bindhu, C.V., Tillack, M.S., et al.: Internal structure and expansion dynamics of laser ablation plumes into ambient gases. J. Appl. Phys. **93**, 2380–2388 (2003). https://doi.org/10.1063/1.1544070

Hashida, M., Mishima, H., Tokita, S., Sakabe, S.: Non-thermal ablation of expanded polytetrafluoroethylene with an intense femtosecond-pulse laser. Opt. Express **17**, 13116 (2009). https://doi.org/10.1364/oe.17.013116

Herziger, G., Kreutz, E.W.: Trends in materials processing with laser radiation. Semicond. Lasers **1025**, 2–9 (1989). https://doi.org/10.1117/12.950189

Hong, S., Lee, H., Yeo, J., Ko, S.H.: Digital selective laser methods for nanomaterials: from synthesis to processing. Nano Today **11**, 547–564 (2016). https://doi.org/10.1016/j.nantod.2016.08.007

Ismail, R.A., Mousa, A.M., Shaker, S.S.: Pulsed laser deposition of nanostructured MgO film: effect of laser fluence on the structural and optical properties. Mater. Res. Express **6**, 075007 (2019). https://doi.org/10.1088/2053-1591/ab1208

Jaber, N., Wolfman, J., Daumont, C., et al.: Laser fluence and spot size effect on compositional and structural properties of $BiFeO_3$ thin films grown by pulsed laser deposition. Thin Solid Films **634**, 107–111 (2017). https://doi.org/10.1016/j.tsf.2017.05.003

Jamaludin, N., Chaudhary, K.T., Haider, Z., et al.: Effect of laser energy and wavelength on average size of gold nanoparticles synthesized by pulsed laser ablation in deionized water. J. Phys. Conf. Ser. **1484**, 012029 (2020). https://doi.org/10.1088/1742-6596/1484/1/012029

Joe, D.J., Kim, S., Park, J.H., et al.: Laser-material interactions for flexible applications. Adv. Mater. **29**, 1606586 (2017). https://doi.org/10.1002/adma.201606586

Kamaruddin, N.H., Bakar, A.A.A., Mobarak, N.N., et al.: Binding affinity of a highly sensitive Au/Ag/Au/Chitosan-graphene oxide sensor based on direct detection of Pb^{2+} and Hg^{2+} ions. Sensors (Switzerland) **17**, 2277 (2017). https://doi.org/10.3390/s17102277

Kareem, S.M., et al.: Cr_2O_3:TiO_2 nanostructure thin film prepared by pulsed laser deposition technique as NO_2 gas sensor. Baghdad Sci. J. **17**, 0329 (2020). https://doi.org/10.21123/bsj.2020.17.1(Suppl.).0329

Kargozar, S., Mozafari, M.: Nanotechnology and nanomedicine: start small, think big. Mater. Today Proc. **5**, 15492–15500 (2018). https://doi.org/10.1016/j.matpr.2018.04.155

Kautek, W.: Formation of Y–Ba–Cu–Oxide thin films by pulsed laser deposition: a comparative study in the UV, visible and IR range. Thin Solid Films **191**, 317–334 (1990)

Kuppusami, P., Raghunathan, V.S.: Status of pulsed laser deposition: challenges and opportunities. Surf. Eng. **22**, 81–83 (2006). https://doi.org/10.1179/174329406X98502

Li, G., Kim, T.W., Inoue, S., et al.: Epitaxial growth of single-crystalline AlN films on tungsten substrates. Appl. Phys. Lett. **89**, 241905 (2006). https://doi.org/10.1063/1.2404588

Lin, J.L., Wang, Z.J., Zhao, X., et al.: Microstructures and ferroelectric properties of $PbTiO_3$/$PbZrO_3$ superlattices deposited by pulse laser deposition. Ceram. Int. **44**, 20664–20670 (2018). https://doi.org/10.1016/j.ceramint.2018.08.059

Liu, C., Mao, X.L., Mao, S.S., et al.: Nanosecond and femtosecond laser ablation of brass: particulate and ICPMS measurements. Anal. Chem. **76**, 379–383 (2004). https://doi.org/10.1021/ac035040a

Liu, H., Lin, W., Hong, M.: Hybrid laser precision engineering of transparent hard materials: challenges, solutions and applications. Light Sci. Appl. **10**, 1–23 (2021). https://doi.org/10.1038/s41377-021-00596-5

Lu, Y., Huang, G., Wang, S., et al.: A review on diamond-like carbon films grown by pulsed laser deposition. Appl. Surf. Sci. **541**, 148573 (2021). https://doi.org/10.1016/j.apsusc.2020.148573

Lyu, J., Estandía, S., Gazquez, J., et al.: Control of polar orientation and lattice strain in epitaxial $BaTiO_3$ films on silicon. ACS Appl. Mater. Interfaces **10**, 25529–25535 (2018). https://doi.org/10.1021/acsami.8b07778

Menazea, A.A., Awwad, N.S.: Pulsed Nd:YAG laser deposition-assisted synthesis of silver/copper oxide nanocomposite thin film for 4-nitrophenol reduction. Radiat. Phys. Chem. **177**, 109112 (2020). https://doi.org/10.1016/j.radphyschem.2020.109112

Menazea, A.A., Abdelbadie, S.A., Ahmed, M.K.: Manipulation of AgNPs coated on selenium/carbonated hydroxyapatite/ε-polycaprolactone nano-fibrous via pulsed laser deposition for wound healing applications. Appl. Surf. Sci. **508**, 145299 (2020a). https://doi.org/10.1016/j.apsusc.2020.145299

Menazea, A.A., Mostafa, A.M., Al-Ashkar, E.A.: Impact of CuO doping on the properties of CdO thin films on the catalytic degradation by using pulsed-laser deposition technique. Opt. Mater. **100**, 109663 (2020b). https://doi.org/10.1016/j.optmat.2020.109663

Mirjolet, M., Sánchez, F., Fontcuberta, J.: High carrier mobility, electrical conductivity, and optical transmittance in epitaxial $SrVO_3$ thin films. Adv. Funct. Mater. **29**, 1–7 (2019). https://doi.org/10.1002/adfm.201808432

Mostafa, A.M., Menazea, A.A.: Laser-assisted for preparation ZnO/CdO thin film prepared by pulsed laser deposition for catalytic degradation. Radiat. Phys. Chem. **176**, 109020 (2020). https://doi.org/10.1016/j.radphyschem.2020.109020

Nicolaou, C., Zacharia, A., Delimitis, A., et al.: Single-step growth of high quality CIGS/CdS heterojunctions using pulsed laser deposition. Appl. Surf. Sci. **511**, 145547 (2020). https://doi.org/10.1016/j.apsusc.2020.145547

Nishikawa, H., Hasegawa, T., Miyake, A., et al.: Effect of laser fluence and ambient gas pressure on surface morphology and chemical composition of hydroxyapatite thin films deposited using pulsed laser deposition. Appl. Surf. Sci. **427**, 458–463 (2018). https://doi.org/10.1016/j.apsusc.2017.08.129

Ogugua, S.N., Ntwaeaborwa, O.M., Swart, H.C.: Latest development on pulsed laser deposited thin films for advanced luminescence applications. Coatings **10**, 1–22 (2020). https://doi.org/10.3390/coatings10111078

Ojeda-G-P, A., Schneider, C.W., Döbeli, M., et al.: The flip-over effect in pulsed laser deposition: is it relevant at high background gas pressures? Appl. Surf. Sci. **357**, 2055–2062 (2015a). https://doi.org/10.1016/j.apsusc.2015.09.184

Ojeda-G-P, A., Schneider, C.W., Döbeli, M., et al.: Angular distribution of species in pulsed laser deposition of $La_xCa_{1-x}MnO_3$. Appl. Surf. Sci. **336**, 150–156 (2015b). https://doi.org/10.1016/j.apsusc.2014.10.089

Ojeda-G-P, A., Schneider, C.W., Döbeli, M., et al.: Plasma plume dynamics, rebound, and recoating of the ablation target in pulsed laser deposition. J. Appl. Phys. **121**, 1–13 (2017). https://doi.org/10.1063/1.4979780

Ojeda-G-P, A., Döbeli, M., Lippert, T.: Influence of plume properties on thin film composition in pulsed laser deposition. Adv. Mater. Interfaces **5**, 1–16 (2018). https://doi.org/10.1002/admi.201701062

Packwood, D.M., Shiraki, S., Hitosugi, T.: Effects of atomic collisions on the stoichiometry of thin films prepared by pulsed laser deposition. Phys. Rev. Lett. **111**, 1–5 (2013). https://doi.org/10.1103/PhysRevLett.111.036101

Pazokian, H., Jelvani, S., Barzin, J., et al.: Effect of spot size on cone formation in a XeCl laser ablation of polyethersulfone films. Opt. Commun. **284**, 363–367 (2011). https://doi.org/10.1016/j.optcom.2010.08.058

Prasad, A.V., Misra, P., Ahirwar, G.: A study on structural and optical properties of $Mg_xZn_{1-x}O$ thin films using pulsed laser deposition (PLD). Res. J. Phys. Sci. **1**, 11–14 (2013)

Rashed, S.H., Haider, A.J., Younis, S.: Preparation and characterization of (TiO_2–SnO_2) thin films by pulsed laser deposition. Part B Eng. Technol. J. **32**, 3–4 (2014)

Rau, J.V., Cacciotti, I., De Bonis, A., et al.: Fe-doped hydroxyapatite coatings for orthopedic and dental implant applications. Appl. Surf. Sci. **307**, 301–305 (2014). https://doi.org/10.1016/j.apsusc.2014.04.030

Robert, D.: Laser Processing and Chemistry, pp. 106–112. Springer, Berlin (2011)

Rodkey, N., Kaal, S., Sebastia-Luna, P., et al.: Pulsed laser deposition of $Cs_2AgBiBr_6$: from mechanochemically synthesized powders to dry, single-step deposition. Chem. Mater. **33**, 7417–7422 (2021). https://doi.org/10.1021/acs.chemmater.1c02054

Rodríguez-Hernández, P.E., Quiñones-Galván, J.G., Meléndez-Lira, M., et al.: Effect of laser fluence on structural and optical properties of Cu_xS films grown by pulsed laser deposition at different wavelengths. Mater. Res. Express **7**, 015908 (2020). https://doi.org/10.1088/2053-1591/ab663d

Salih, A.A., Nazar, A., Haider, A.J.: Antibacterial activity of ZnO nanoparticle prepared by pulsed laser ablation in liquid for biological sensor. In: Proceedings: International Conference on Developments in eSystems Engineering, DeSE October-20, pp. 726–729 (2019). https://doi.org/10.1109/DeSE.2019.00135

Sambri, A., Aruta, C., Di Gennaro, E., et al.: Effects of oxygen background pressure on the stoichiometry of a $LaGaO_3$ laser ablation plume investigated by time and spectrally resolved two-dimensional imaging. J. Appl. Phys. **119**, 125301 (2016). https://doi.org/10.1063/1.4943589

Sangwaranatee, N.W., Sangwaranatee, N., Chananonnawathorn, C., Horprathum, M.: Influence on distance between substrate and target on the properties of CuO thin film prepared by DC reactive magnetron sputtering. Mater. Today Proc. **5**, 13900–13903 (2018). https://doi.org/10.1016/j.matpr.2018.02.037

Schou, J., Toftmann, B., Amoruso, S.: Dynamics of a laser-produced silver plume in an oxygen background gas. High-Power Laser Ablation V **5448**, 110–120 (2004). https://doi.org/10.1117/12.548684

Shaheen, M.E., Gagnon, J.E., Fryer, B.J.: Excimer laser ablation of aluminum: influence of spot size on ablation rate. Laser Phys. **26**, 116102 (2016). https://doi.org/10.1088/1054-660X/26/11/116102

Shen, J., Gai, Z., Kirschner, J.: Growth and magnetism of metallic thin films and multilayers by pulsed-laser deposition. Surf. Sci. Rep. **52**, 163–218 (2004)

Singh, R.K., Narayan, J.: A novel method for simulating laser-solid interactions in semiconductors and layered structures. Mater. Sci. Eng. B **3**, 217–230 (1989). https://doi.org/10.1016/0921-5107(89)90014-7
Smith, H.M., Turner, A.F.: Vacuum deposited thin films using a ruby laser. Appl. Opt. **4**, 3–4 (1965)
Song, Y., Li, Z., Li, H., et al.: Epitaxial growth and characterization of high quality Bi_2O_2Se thin films on $SrTiO_3$ substrates by pulsed laser deposition. Nanotechnology **31**, 165704 (2020). https://doi.org/10.1088/1361-6528/ab6686
Taha, B.A.: Perspectives of photonics technology to diagnosis COVID–19 viruses: a short review. J. Appl. Sci. Nanotechnol. **1**, 1–6 (2021). https://doi.org/10.53293/jasn.2021.11016
Taha, B.A., Al, M.Y., Mokhtar, M.H.H., et al.: An analysis review of detection coronavirus disease 2019 (Covid-19) based on biosensor application. Sensors (Switzerland) **20**, 1–29 (2020). https://doi.org/10.3390/s20236764
Taha, B.A., Ali, N., Sapiee, N.M., et al.: Comprehensive review tapered optical fiber configurations for sensing application: trend and challenges. Biosensors **11**, 253 (2021a). https://doi.org/10.3390/bios11080253
Taha, B.A., Al Mashhadany, Y., Bachok, N.N., et al.: Detection of covid-19 virus on surfaces using photonics: challenges and perspectives. Diagnostics **11**, 1119 (2021b). https://doi.org/10.3390/diagnostics11061119
Taha, B.A., Min, L.: Morphological features and divergence of SARS-CoV_2 and SARS-CoV virus using TEM images. 1–21 (2022)
Takahashi, T., Tani, S., Kuroda, R., Kobayashi, Y.: Precision measurement of ablation thresholds with variable pulse duration laser. Appl. Phys. A Mater. Sci. Process. **126**, 1–7 (2020). https://doi.org/10.1007/s00339-020-03754-5
Torrisi, L., Andò, L., Ciavola, G., et al.: Angular distribution of ejected atoms from Nd:YAG laser irradiating metals. Rev. Sci. Instrum. **72**, 68–72 (2001). https://doi.org/10.1063/1.1328404
Treece, R.E., Horwitz, J.S., Claassen, J.H., Chrisey, D.B.: Pulsed laser deposition of high-quality NbN thin films. Appl. Phys. Lett. **65**, 2860–2862 (1994). https://doi.org/10.1063/1.112516
Ursu, C., Nica, P., Focsa, C.: Excimer laser ablation of graphite: the enhancement of carbon dimer formation. Appl. Surf. Sci. **456**, 717–725 (2018). https://doi.org/10.1016/j.apsusc.2018.06.217
Venkatesan, T.: Pulsed laser deposition: invention or discovery? J. Phys. D Appl. Phys. **47**, 3–10 (2014). https://doi.org/10.1088/0022-3727/47/3/034001
Vinodkumar, R., Jeena, V., Jiji, V., et al.: Structural, optical and dielectric properties of gadolinium incorporated laser ablated ZnO thin films. Optik **174**, 274–281 (2018). https://doi.org/10.1016/j.ijleo.2018.08.074
Wang, Z.B., Hong, M.H., Luk'yanchuk, B.S., et al.: Angle effect in laser nanopatterning with particle-mask. J. Appl. Phys. **96**, 6845–6850 (2004). https://doi.org/10.1063/1.1786652
Yu, C., Zhou, W., Chang, H., Chen, Y.: Experimental research on impulse coupling characteristics and plasma plume dynamics of a nanosecond pulsed laser irradiated aluminum target. IEEE Access **8**, 205272–205281 (2020). https://doi.org/10.1109/ACCESS.2020.3037302
Yuan, B.S., Zhang, Y., Zhang, W., et al.: The effect of spot size combination mode on ablation morphology of aluminum alloy by millisecond-nanosecond combined-pulse laser. Materials **11**, 1419 (2018). https://doi.org/10.3390/ma11081419
Zhang, J., Xue, W., Su, T., et al.: Nanoscale magnetization reversal by magnetoelectric coupling effect in $Ga_{0.6}Fe_{1.4}O_3$ multiferroic thin films. ACS Appl. Mater. Interfaces **13**, 18194–18201 (2021). https://doi.org/10.1021/acsami.0c21659
Zhao, L., Liu, Z., Chen, D., et al.: Laser Synthesis and Microfabrication of Micro/Nanostructured Materials Toward Energy Conversion and Storage. Springer, Singapore (2021)
Zhigilei, L.V.: Dynamics of the plume formation and parameters of the ejected clusters in short-pulse laser ablation. Appl. Phys. A Mater. Sci. Process. **76**, 339–350 (2003). https://doi.org/10.1007/s00339-002-1818-5

Authors and Affiliations

Adawiya J. Haider[1] · Taif Alawsi[2] · Mohammed J. Haider[3] · Bakr Ahmed Taha[4] · Haydar Abdulameer Marhoon[5,6]

Taif Alawsi
taif.alawsi@alayen.edu.iq

Mohammed J. Haider
140120@uotechnology.edu.iq

Bakr Ahmed Taha
p103537@siswa.ukm.edu.my

Haydar Abdulameer Marhoon
haydar@alayen.edu.iq

1 Department of Applied Sciences, Laser Branch, University of Technology-Iraq, Baghdad, Iraq

2 Technical Engineering College, Al-Ayen University, Thi-Qar, Iraq

3 Electrical Engineering Department, University of Technology-Iraq, Baghdad, Iraq

4 UKM—Department of Electrical, Electronic and Systems Engineering, Faculty of Engineering and Built Environment, Universiti Kebangsaan Malaysia (UKM), 43600 Bangi, Malaysia

5 Information and Communication Technology Research Group, Al-Ayen University, Thi-Qar, Iraq

6 College of Computer Sciences and Information Technology, University of Kerbala, Kerbala, Iraq